Available online at www.sciencedirect.com

ScienceDirect

Procedia Engineering 102 (2015) 986 – 995

Procedia Engineering

www.elsevier.com/locate/procedia

The 7th World Congress on Particle Technology (WCPT7)

Particle concentration measurement and flow regime identification in multiphase pipe flow using a generalised dual-frequency inversion method

Hugh P. Rice[a,*], Michael Fairweather[a], Jeffrey Peakall[b], Timothy N. Hunter[a], Bashar Mahmoud[a], Simon R. Biggs[a]

[a]*School of Process, Environmental and Materials Engineering, University of Leeds, Leeds LS2 9JT, United Kingdom*
[b]*School of Earth and Environment, University of Leeds, Leeds LS2 9JT, United Kingdom*

Abstract

An acoustic particle concentration measurement method, originally developed for marine sediment, in which the backscattered energy received by emitter-receiver transducers in the megahertz range is used to construct concentration profiles in suspensions of solid particles in a carrier fluid is applied to suspensions of general engineering interest. Four particle species with range of densities and sizes are used. Concentration profiles in horizontal, turbulent pipe flow at a Reynolds number of 50,000 and three nominal volume fractions are presented for each particle species, using experimentally determined acoustic coefficients, in order to isolate the influence of particle size and density on transport and settling in solid-liquid multiphase flows. It is clear from the results that the method allows the degree of segregation in real suspensions and slurries to be measured, and has a range of potential applications in the nuclear and minerals processing industries, for example. Lastly, the limiting conditions of the method are explored through the concept of an acoustic penetration depth.

Selection and peer-review under responsibility of Chinese Society of Particuology, Institute of Process Engineering, Chinese Academy of Sciences (CAS)

Keywords: Acoustic backscatter; sediment transport; scattering; attenuation; instrumentation.

* Corresponding author. Tel.: +44-113-343-2351; fax: +44-113-343-2384.
E-mail address: h.p.rice@leeds.ac.uk

Selection and peer-review under responsibility of Chinese Society of Particuology, Institute of Process Engineering, Chinese Academy of Sciences (CAS)
doi:10.1016/j.proeng.2015.01.221

1. Introduction

Solid-liquid suspension flow can been categorised as follows: non-settling, where the solids are fully suspended; unhindered-settling, where the (dilute) solids can settle freely due to gravity; or hindered-settling, where the settling of solids is hindered by upward-moving fluid, as dictated by the conservation of mass [1-3]. Five flow regimes for suspensions can alternatively be identified: (pseudo-)homogeneous, where the solid phase is fully suspended and there is no cross-sectional variation in the particle concentration; heterogeneous, where the particle concentration varies across the pipe diameter; flow with a moving bed or "saltation" flow, where a proportion of the solid fraction has formed a moving bed; flow with a stationary bed, in which at least part of the sediment is stationary; and plug flow, where the particles occupy the whole diameter of the conduit and move together by sliding [1]. Flow regimes can be delineated by transition velocities, with fully suspended and bed-forming flows being separated by the critical deposition velocity [4, 5].

The aim of this study is to investigate the influence of particle size and nominal concentration on the local concentration profile through a vertical cross-section at flow velocities above the critical deposition velocity, that is, in fully suspended flows. A summary of some prominent studies of concentration profiles in heterogeneous suspensions in pipes and channels follows, where Re is the Reynolds number and is defined as follows:

$$\mathrm{Re} = \frac{U_b D}{v}, \tag{1}$$

where U_b is the bulk flow velocity in the axial direction, D is the internal pipe diameter and v is the kinematic viscosity of the fluid.

A model for the cross-sectional particle concentration in pipe and channel flows was developed by Karabelas [6], who found very good agreement with his own experimental results (spherical plastic particles in kerosene, oil, and mixtures of the two) and the sand-in-water results of Durand [7]. The "two-layer" model of Gillies *et al.* [8] incorporates a layer of suspended, buoyant particles ("fines") and carrier fluid, and a bed comprised of two components, a "contact load", through which energy is dissipated by friction with the wall, and a "suspended load", whose weight is held by the carrier fluid. The model was tested against experiments and compared well with experimental concentration profile data for suspensions of coarse sand from Gillies and Shook [9], and has been extended to higher volume fractions close to the critical deposition velocity (volume fraction $\phi > 35\%$ or so) [10] and higher flow velocities [11]. The particle concentration was found to vary linearly with height above stationary beds by Pugh and Wilson [12], and Admiraal and García [13] measured the particle concentration above a sand bed in a water channel using a forerunner of the model used in this study. Researchers at the Saskatchewan Research Council (SRC) [11] measured sand concentration profiles in pipe flow, and their two-layer model [14] was able to accurately predict the proportion of suspended solids in high-concentration flows.

Ekambara *et al*. [15] found close agreement in terms of concentration, velocity and pressure drop between their modelling and experimental results and numerical data from the literature. In one of a number of related papers, Matoušek [16] presented concentration profiles in flows with sand beds and modelled the solid fraction as comprising three layers – a stationary bed, a shear layer and a fully suspended region – in comparison to the two-layer model of Gillies *et al*. [8, 11]. Furlan *et al*. [17] found reasonable agreement between experimental and numerical results with spherical glass beads in water using an ultrasonic measurement technique. Capecelatro and Desjardins [18] performed fully coupled numerical simulations of glass-like particles at two flow velocities; particles were tracked individually and excellent agreement was found between the numerical results and an experimental dataset from the literature [19]. The model of Kaushal and Tomita [20], which was based on an earlier approach [21], found very good agreement with several other studies [9, 16, 22].

This paper has several objectives. First, lower-concentration flows are investigated, which are of particular interest for several reasons, both industrially and in terms of fluid mechanics, and span the boundary between dilute and concentrated flows, at which fluid-particle and particle-particle interactions begin to influence the flow behaviour. It is therefore surprising to note that concentration profile data are scarce at relatively low particle concentrations (*i.e.* up to a few per cent by volume), although some are available at higher concentrations [6, 11, 15, 23] and in the presence of a settled bed [12, 16].

Second, a model relating the backscattered acoustic signal received by an emitter-receiver transducer to the physical and acoustic properties of suspended solid particles [24] has been modified [25] to be applicable to suspensions of particles with arbitrary properties of engineering interest. Values of the backscattering and attenuation coefficients for four particle types (two spherical glass, two non-spherical plastic), and a novel method for measuring them, were presented. With these measured coefficients, some concentration profiles in horizontal pipe flow were computed for validation purposes using a dual-frequency concentration inversion method [24, 26], which avoids the numerical instabilities inherent in several other inversions in the far field. In this paper, a range of concentration profiles normalised by nominal concentrations is presented.

Third, an acoustic method was chosen that avoids as many problems as possible that are present in other methods (such as those described earlier), namely: suitable for non-marine flows – *i.e.* those of real, general engineering interest; has high spatial and temporal resolution and does not rely on time-consuming, point-wise measurements or physical sampling; is low-cost; is easy to deploy and can be operated non-intrusively; does not have computationally demanding post-processing requirements; and is as safe as possible, preferably not employing ionizing radiation.

The paper is structured as follows: (a) brief summaries of the Thorne and Hanes [24] and Hurther *et al*. [26] models are given in Section 2; (b) the method of operation of the *UVP-DUO* instrument and the pipe flow loop, and the physical properties of the particle species, are summarised in Section 3; and (c) a full set of concentration profiles at four nominal particle volume fractions above the critical deposition velocity (all at Re ≈ 50,000) are presented in Section 4, as well as a derivation of an acoustic penetration depth, through which the limitations of the method are quantified in the general case and *via* the application-specific maximum measurable concentration.

2. Concentration inversion methods in solid-liquid suspensions

The attenuation-based acoustic model of Thorne and Hanes [24] and Hurther *et al*. [26] is described in this section, as it is used as the basis of this study. The reader is referred to Rice [25] for a more thorough description. The RMS voltage, V, excited in an ultrasonic transducer by backscattered energy depends on the mass concentration of suspended particles, M, and the distance from the transducer, r, as follows [24]:

$$V = \frac{k_s k_t}{\psi r} M^{1/2} e^{-2r\alpha}, \tag{2}$$

where α is the attenuation due to both scattering and absorption, and has components contributed by the fluid and solid phases, such that

$$\alpha = \alpha_w + \alpha_s, \tag{3}$$

where α_w and α_s are the attenuation due to water and solid particles, respectively; k_s is the sediment backscatter constant and incorporates the backscattering properties of the particles; and k_t is a system constant. As discussed by Rice [25], here k_s and k_t are combined and expressed as the backscattering and system coefficient, K, such that

$$K = k_s k_t. \tag{4}$$

The particle concentration, M, is referred to in this study alongside the volume fraction, ϕ, which are related as follows:

$$\phi = \frac{M}{\rho_s}, \tag{5}$$

where ρ_s is the material density of the solid phase. The near-field correction factor, ψ, tends to unity in the far field, more details of which have been given by Downing *et al.* [27]. The attenuation due to water, α_w, is calculated using the expression given by Ainslie and McColm [28], and the attenuation due to the solid phase, α_s, is found in the general case – in which both M and the particle attenuation coefficient, ξ, vary with distance from the transducer – using the following integral:

$$\alpha_s = \frac{1}{r}\int_0^r \xi(r')\, M(r')\mathrm{d}r'. \tag{6}$$

The coefficients K and ξ therefore incorporate the acoustic properties of the suspended particles. However, published data for K and ξ exist only for quartz sand [29]. A novel method for measuring K and ξ for arbitrary materials was presented by Rice [25], and the measured values for spherical glass and non-spherical plastic particles are summarised in Table 1. A brief reiteration of the method follows. First, Equation (6) is simplified for the case of a homogeneous suspension, in which neither M, the particle size distribution nor, therefore, ξ vary with distance, so that

$$\alpha_{sh} = \xi_h M, \tag{7}$$

where the subscript h denotes homogeneity. Then, once the range-corrected echo amplitude, G, has been defined as follows:

$$G = \ln(\psi r V), \tag{8}$$

Equation (2) can be rearranged so that after taking the second derivative with respect to r and M, an expression for the attenuation coefficient in homogeneous suspensions, ξ_h, is obtained:

$$\xi_h = -\frac{1}{2}\frac{\partial}{\partial M}\left[\frac{\partial}{\partial r}[\ln(\psi r V)]\right] = -\frac{1}{2}\frac{\partial^2 G}{\partial M \partial r}. \tag{9}$$

By rearranging Equation (2) and noting the identity in Equation (4), the backscatter and system coefficient, K_h, can then be calculated using the measured value of ξ_h, then taking a mean value with respect to both distance, r, and solid-phase mass concentration, M. The method, then, relies on measuring ξ_h *via* the second derivative of the range-corrected echo amplitude, G, with respect to r and M. In practice, this means that the suspensions used in the calibration procedure described above must have known, homogeneous concentrations: it is to homogeneity in that specific context that the subscript h refers in ξ_h and K_h, and not to the suspensions in which the coefficients can ultimately be used. On the contrary, and as described below, once measured, the coefficients can be used to reconstruct the concentration field in arbitrary suspensions.

The purpose of a concentration inversion method is to rewrite Equation (2) so that the mass concentration of particles, M, is expressed in terms of the received RMS voltage, V, and the other known quantities, including K and ξ. However, such inversions are difficult because M appears more than once in Equations (2), (3) and (6), and many implicit and explicit inversion methods become numerically unstable in the far field [24]. However, in this study, an explicit dual-frequency inversion method [26, 30] that avoids such instabilities is employed: the particle concentration can be calculated at any position from the transducer independently. In this method, M is obtained by algebraic manipulation of Equation (2) as follows:

$$M = J_1^{(1-\xi_1/\xi_2)^{-1}} J_2^{(1-\xi_2/\xi_1)^{-1}}, \tag{10}$$

where J is as defined below and the subscripts 1 and 2 refer to the two frequencies at which voltage profiles must be measured:

$$J(r) \equiv M e^{-4\int_0^r \xi(r')M(r')\mathrm{d}r'} = V^2(r)/\Phi^2(r), \tag{11}$$

where V is the recorded RMS voltage and Φ^2 contains the known quantities and is as follows:

$$\Phi^2 \equiv \left(\frac{K}{\psi r}\right)^2 e^{-4r\alpha_w}. \tag{12}$$

3. Materials and methods

The physical and acoustic properties of the four particle species that were used in this study are summarised in Table 1. The species were chosen because they span a range of sizes, densities and shapes, and therefore have a wide range of scattering and absorption properties. The methods and apparatus used to determine those properties were summarised in Section 2 and are described more fully by Rice [25]. An ultrasonic system, consisting of a *UVP-DUO* signal processor (Met-Flow, Switzerland) and two transducers operating at 2 and 4 MHz, was chosen as the principal measurement instrument for the present study, based on a number of criteria (versatility, low cost, portability, ease of operation and unrestrictive computational requirements). The two transducers were mounted on a straight, horizontal test section of a recirculating pipe flow loop (see Fig. 1) with an inner diameter D = 42.6 mm. A variable-speed centrifugal pump was used to control the flow rate, a mixer with impeller to maintain a stable suspension in the mixing tank (nominal capacity 100 litres) and an electromagnetic flow meter to display the flow rate. The flow loop was filled with suspensions of each of the four particle species listed in Table 1 at several known, weighed concentrations and run at a Reynolds number of Re ≈ 50,000 ($U_b \approx 1.2$ m s^{-1}). Data from pairs of runs at the two ultrasonic frequencies were recorded and combined using Equation (10), in which J_1, J_2 and M are functions of distance, r, from the transducer, yielding concentration profiles along a vertical cross-section.

Table 1. Physical and acoustic properties of particle species. All supplied by Guyson International, Ltd., U.K.

Particle species	Small glass	Large glass	Small plastic	Large plastic
Shape	Spherical	Spherical	Jagged	Jagged
d_{50} (μm)	41.0	77.0	468	691
ρ (10^3 kg m^{-3})	2.45	2.46	1.54	1.52
K_{h1} (2 MHz)	0.00229	0.00363	0.0100	0.0163
K_{h2} (4 MHz)	0.00430	0.00699	0.0239	0.0182
ξ_{h1} (2 MHz)	0.0182	0.0212	0.627	1.34
ξ_{h2} (4 MHz)	0.0694	0.135	2.74	2.73

Legend: d_{50} is median particle size; ρ is density; k is ultrasonic wavenumber; a is particle radius (*i.e.* $d_{50}/2$); K_h is backscattering and system constant; ξ_h is attenuation coefficient; subscripts 1 and 2 refer to ultrasonic frequency f = 2 and 4 MHz, respectively.

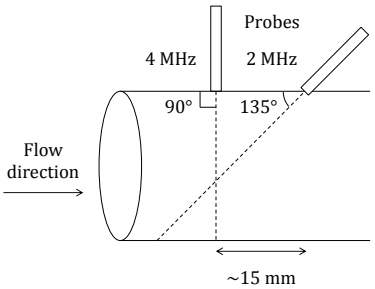

Fig. 1. Probe mounting geometry schematic. Inner diameter, D = 42.6 mm; entry length, L = 3.2 m.

For every run in the pipe flow loop, n = 2,500 samples were taken. The system-applied gain and digitisation constant were removed from the raw data in MATLAB, and a three-sigma noise filter applied, to give the RMS voltage, V. As is clear from Fig. 1, the measurement points for each transducer were not co-located, so linear interpolation of one dataset (the 2 MHz data) in each pair of runs was performed. The common axis was chosen to be the perpendicular upward distance from the pipe centreline, y'.

4. Results and discussion

The influence of attenuation on computed concentration is explored in Section 4.1, and expressions for an acoustic penetration depth, δ_p, and an application-specific limiting particle concentration, M_{lim}, are derived and discussed. Concentration profiles computed according to the method described in Section 2 using Equation (10) are presented at Re ≈ 50,000 at three nominal concentrations for all four particle species in Section 4.

4.1. Penetration depth and limiting concentration

The presence of attenuation by suspended particles is a requirement of the model, but excessive attenuation will cause the acoustic signal to be extinguished (by scattering and absorption) before a proportion of it reaches the transducer *via* backscattering. The physical arguments and scoping calculations presented in this section are intended as suggestions for designing future experiments: a balance must generally be found between the strength of the received signal and the maximum distance over which data can be gathered. By inspection of Equations (2), (3) and (7) an acoustic penetration depth, δ_p, over which the acoustic signal will be attenuated by a factor of e^{-1}, can be defined such that

$$\delta_p = \frac{1}{\xi_h M}. \tag{13}$$

The attenuation coefficient, ξ_h, is known for all particle species (Table 1), so δ_p can be calculated for the nominal concentrations used in this study, *i.e.* ϕ_w = 0.5, 1 and 3 % (M_w = 12.4, 24.7 and 72.8 kg m^{-3} for the glass species; M_w = 7.46, 14.9 and 43.7 kg m^{-3} for the plastic species). The influence of attenuation can also be quantified from the perspective of the limiting concentration, M_{lim}, defined as that at which the desired maximum measurement distance is equal to the penetration depth, *i.e.*:

$$M_{lim} = \frac{1}{\xi \delta_{p,lim}}, \tag{14}$$

where $\delta_{p,lim}$ is the limiting distance corresponding to the limiting concentration. By choosing $\delta_{p,lim} = D$, where D is the inner pipe diameter, the limiting concentration for the flow conditions described in this study can be found, and M_{lim} is given for each particle species in Table 2.

Table 2. Limiting mass concentration, M_{lim} (kg m^{-3}), for all particle species. Nominal mass concentrations, M_w, and volume fractions, ϕ_w, used in this study are also given, for comparison.

	Small glass	Large glass	Small plastic	Large plastic
M_{lim}, 2 MHz	1,290	1,110	37.4	17.5
M_{lim}, 4 MHz	338	174	8.57	8.60
M_w, ϕ_w = 0.5 %	12.4	12.4	7.46	7.46
M_w, ϕ_w = 1 %	24.7	24.7	14.9	14.9
M_w, ϕ_w = 3 %	72.8	72.8	43.7	32.7

It can immediately be seen from Table 2 that M_{lim} is either similar to the nominal concentration, M_w, or exceeds it in several cases. In those cases where $M_{lim} \sim M_w$, the acoustic signal is likely to be attenuated strongly. Where $M_{lim} \ll M_w$, the voltage excited in the transducer may be so low that the particle concentration computed *via* Equation (10) would be either significantly under-predicted or effectively zero, in which cases the method is not reliable. It should also be noted that only the attenuation at the higher acoustic frequency needs to be significant for the computed concentration to be affected, since M depends on both ξ_1 and ξ_2 *via* Equation (10). Attenuation will be significant at the lowest nominal concentration (*i.e.* ϕ_w = 0.5 %) for both plastic particle species, as $M_{lim} \sim M_w$ in those cases, and is likely to overwhelm the acoustic signal at the two higher concentrations (ϕ_w = 1 and 3 %), where $M_{lim} < M_w$. Attenuation may also be significant for the larger glass species at the highest nominal concentration (ϕ_w = 3 %) if a

strong concentration gradient exists towards the lower part of the flow. In the section that follows, the significance of the penetration depths and limiting concentrations presented in this section are discussed further from the perspective of the computed concentration profiles that are presented.

4.2. Particle concentration profiles

Concentration profiles were computed using Equation (10) and the acoustic coefficients given in Table 1 and are presented in this section for each particle species at nominal volume fractions of ϕ_w = 0.5, 1 and 3 % and Re ≈ 50,000 ($U_b \approx 1.2$ m s^{-1}). Profiles for the smaller glass species are shown in Fig. 2(a); for the larger glass in Fig. 2(b); for the smaller plastic in Fig. 3(a); and for the larger plastic in Fig. 3(b). The actual Reynolds numbers and the sampled concentrations, M_s (each is a mean of 3 × 60 ml physical samples taken from the mixing tank) are given in the captions. Note that only the lower half of the flow – *i.e.* $-0.5 < y'/D < 0$ – is shown in the figures, and that the axes are reversed for ease of visualisation. The vertical axis) is normalised by the pipe diameter, D, to give y'/D, and the horizontal axis by the nominal (*i.e.* weighed) mass concentration, M_w (and the nominal volume fraction, ϕ_w) to give M/M_w (which is identical to ϕ/ϕ_w).

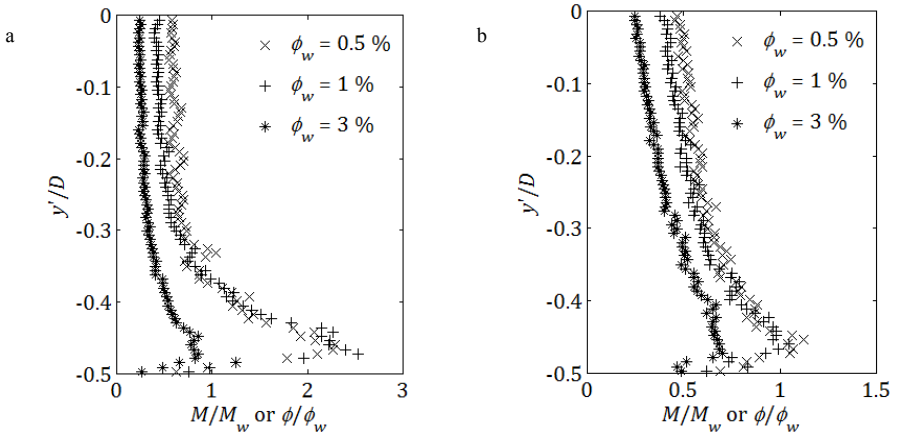

Fig. 2. Normalised concentration, M/M_w, *vs*. reduced distance from centreline, y'/D. (a) Small glass spheres (d_{50} = 41.0 µm), Re = 53,100, 52,700 and 52,100; ϕ_w = 0.5, 1 and 3 %; M_w = 12.4, 24.7 and 72.8 kg m^{-3} (M_s = 13.4, 27.4 and 79.9 kg m^{-3}). (b) Large glass spheres (d_{50} = 77.0 µm), Re = 53,100, 51,600 and 51,100; ϕ_w = 0.5, 1 and 3 %; M_w = 12.4, 24.7 and 72.8 kg m^{-3} (M_s = 13.6, 20.9 and 54.8 kg m^{-3}). Lower half of flow shown.

It should also be noted that the flow rates used in this study greatly exceeded the onset of particle motion: the threshold for incipient particle motion for the smaller plastic particles was found to occur at Re ≈ 6,500 in a study by Rice [25], and is likely to be similar (although marginally higher) for the larger plastic species and significantly higher for both glass species, which are an order of magnitude smaller than the plastic species, though more dense. Moreover, a bed did not form in any of the runs presented in this study: all flow velocities were confirmed to have been above the critical deposition velocity, as measured using a novel method [25]. It is clear that, in all the runs presented here, heterogeneous suspensions were produced. This is as would be expected for a real suspension subject to the gravitational force: M generally increases with downward distance.

As discussed in greater detail elsewhere [25], the transmission of acoustic energy through a solid-liquid suspension is influenced by both absorption and scattering processes. From the frame of reference of a monostatic (*i.e.* single emitter-receiver) transducer, these processes manifest themselves as apparent attenuation and backscatter and are embodied by the attenuation and backscatter/system coefficients, ξ and K, in this study through Equation (2). With these processes borne in mind, the hump-like structures observed in many of the presented concentration profiles can generally be regarded as an indicator of the region over which the backscatter strength of the suspension is overwhelmed by the attenuation due to particles, which depends more strongly on concentration than backscatter does [24] *via* Equation (2).

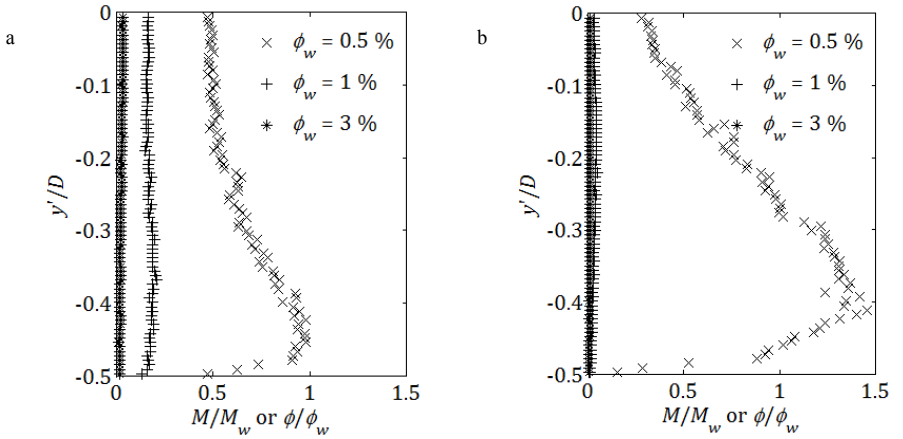

Fig. 3. Normalised concentration, M/M_w, *vs.* reduced distance from centreline, y'/D. (a) Small plastic beads (d_{50} = 468 µm), Re = 52,300, 51,700 and 51,200; ϕ_w = 0.5, 1 and 3 %; M_w = 7.46, 14.9 and 43.7 kg m^{-3} (M_s = 6.71, 17.3 and 40.5 kg m^{-3}). (b) Large plastic beads (d_{50} = 691 µm), Re = 49,700, 50,100 and 48,700; ϕ_w = 0.5, 1 and 3 %; M_w = 7.46, 14.9 and 43.7 kg m^{-3} (M_s = 5.49, 11.2 and 34.3 kg m^{-3}). Lower half of flow shown.

In a suspension of slightly attenuating particles, the concentration, M, would be expected to increase with downward distance through backscattering. In such a suspension, only a solid surface or interface (such as the upper surface of a settled bed) would produce the kind of hump-like structures that are observed (*e.g.* Fig. 2(a): smaller glass species at ϕ_w = 0.5 % and 1 %). However, the source of the humps is more complex in the more general case of a more strongly attenuating, heterogeneous suspension with a moderate nominal particle concentration in which M_{lim} is of the order of M_w over some region of the measurement domain (because the attenuation due to suspended particles, α_s, depends on M in an integral form in general *via* Equation (6)). The dataset at ϕ_w = 3 % for the larger plastic species shown in Fig. 3(b) is a good example of such an intermediate case: a hump can be seen at $y'/D \approx$ -0.4. If the suspension in that dataset were only slightly attenuating, it could be assumed that the hump corresponded to a real structure (*i.e.* a shear layer or a bed), but none was observed during the run, so the position of the hump must correspond to the region over which attenuation overwhelmed backscattering. Based on the models and methods presented here, then, it would be sensible to choose a measurement domain such that the limiting concentration, M_{lim}, approaches or is exceeded by the actual, local concentration, M, at some point within the moving bed/shear layer. In the case of a flow with a stationary bed with a thin or non-existent moving part, this point will coincide with the upper surface of the bed, which acts as a reflective surface so that unambiguous bed depth measurements are possible, if the transducer axis is orientated within a few degrees of normal to the surface [25].

It is to be expected that the plastic particle species would attenuate more strongly than the glass species due to their size [24], and this is borne out in the concentration profiles presented in this study. The expressions for the penetration depth, δ_p, and limiting concentration, M_{lim}, given earlier were evaluated for the experimental conditions used in this study in Table 2 (Section 4.1), from which it can be seen that at f = 4 MHz, M_{lim} = 8.57 and 8.60 kg m^{-3} for the two plastic species, both of which values are close to the lowest nominal concentration, M_w = 7.46 kg m^{-3} (ϕ_w = 0.5). It would be expected that the acoustic signal would be strongly attenuated in those cases. However, the concentration profiles presented in Fig. 3(a) (smaller plastic) and Fig. 3(b) (larger plastic) at ϕ_w = 0.5 % are quite reasonable, though perhaps slightly under-predicted. At ϕ_w = 1 and 3 %, however, the nominal mass concentration (M_w = 14.9 and 43.7 kg m^{-3}, respectively) exceeds the limiting value at f = 4 MHz for both plastic particle types (M_{lim} = 8.57 and 8.60 kg m^{-3} for the small and large plastic, respectively), so it is not surprising that the computed concentration is strongly underestimated throughout the measurement domain for both species at ϕ_w = 3 % (Fig. 3(a) and (b)). The attenuation at ϕ_w = 1 % is not as strong, but the results are nevertheless rendered unreliable by it.

The results for the two plastic species demonstrate the significance of acoustic attenuation on real data. When considered alongside the penetration depth and limiting concentration described in Section 4.2, the results are presented as examples of how acoustically transparent and opaque suspensions can be identified in industrial applications. No concentration-profile data suitable for comparison – in terms of a number of suspension parameters, such as Reynolds number, Archimedes number and/or nominal concentration – could be found in the literature: the available data were found to be either at too high a nominal concentration [6, 11, 15, 23], or had been gathered with

a thick bed present [12, 16]. The paucity of suitable data for comparison is surprising, but suggests that the method described in this study has wide potential for application.

5. Conclusions

A method of using experimentally measured values of the acoustic coefficients ξ_h and K_h in a dual-frequency concentration inversion method was tested and found to be very successful, and the resulting concentration profiles exhibited many of the expected properties. Limitations imposed on the method by acoustic attenuation due to suspended particles were quantified, and weakly and strongly attenuating suspensions were delineated by the acoustic penetration depth, δ_p, and the limiting concentration, M_{lim}. The latter parameter was contrived to be specific to a particular geometry or application, and so the expressions presented for δ_p and M_{lim} can be used to identify the most suitable acoustic frequencies for particular flow conditions and particle properties. The method used in this study, which is novel as a whole, has great potential in a range of engineering industries where chemical, radiological or other hazards render *in-situ* characterisation of flowing or settling suspensions difficult.

Acknowledgements

This study is based on part of the Ph.D. thesis of H.P. Rice ("Transport and deposition behaviour of model slurries in closed pipe flow", University of Leeds, 2013). The authors wish to thank the Engineering and Physical Sciences Research Council for their financial support of the work reported in this paper under EPSRC Grant EP/F055412/1, "DIAMOND: Decommissioning, Immobilisation and Management of Nuclear Wastes for Disposal". The authors also thank Peter Dawson, Gareth Keevil and Russell Dixon for their technical assistance.

References

[1] C.T. Crowe, Multiphase Flow Handbook, CRC Press, Taylor & Francis, Boca Raton, 2006.
[2] P. Doron, D. Barnea, Pressure drop and limit deposit velocity for solid-liquid flow in pipes, Chem. Eng. Sci. 50 (1995) 1595-1604.
[3] E.J. Wasp, J.P. Kenny, R.L. Gandhi, Solid-Liquid Flow Slurry Pipeline Transportation, Trans-Tech Publications, Clausthal, 1977.
[4] F.B. Soepyan, S. Cremaschi, C. Sarica, H.J. Subramani, G.E. Kouba, Solids transport models comparison and fine-tuning for horizontal, low concentration flow in single-phase carrier fluid, AlChE J. 60 (2014) 76-112.
[5] A.R. Oroskar, R.M. Turian, The critical velocity in pipeline flows of slurries, AlChE J. 26 (1980) 550-558.
[6] A.J. Karabelas, Vertical distribution of dilute suspensions in turbulent pipe flow, AlChE J. 23 (1977) 426-434.
[7] R. Durand, E. Condolios, The hydraulic transport of coal and solids materials in pipes, in Colloquium on the Hydraulic Transport of Coal, National Coal Board, London, 1952.
[8] R.G. Gillies, C.A. Shook, K.C. Wilson, An improved two layer model for horizontal slurry pipeline flow, Can. J. Chem. Eng. 69 (1991) 173-178.
[9] R.G. Gillies, C.A. Shook, Concentration distributions of sand slurries in horizontal pipe flow, Particul. Sci. Technol. 12 (1994) 45-69.
[10] R.G. Gillies, J. Schaan, R.J. Sumner, M.J. McKibben, C.A. Shook, Deposition velocities for Newtonian slurries in turbulent flow, Can. J. Chem. Eng. 78 (2000) 704-708.
[11] R.G. Gillies, C.A. Shook, J.H. Xu, Modelling heterogeneous slurry flows at high velocities, Can. J. Chem. Eng. 82 (2004) 1060-1065.
[12] F.J. Pugh, K.C. Wilson, Velocity and concentration distributions in sheet flow above plane beds, J. Hydraul. Eng.-ASCE 125 (1999) 117-125.
[13] D.M. Admiraal, M.H. García, Laboratory measurement of suspended sediment concentration using an Acoustic Concentration Profiler (ACP), Exp. Fluids 28 (2000) 116-127.
[14] R.G. Gillies, C.A. Shook, Modelling high concentration settling slurry flows, Can. J. Chem. Eng. 78 (2000) 709-716.
[15] K. Ekambara, R.S. Sanders, K. Nandakumar, J.H. Masliyah, Hydrodynamic simulation of horizontal slurry pipeline flow using ANSYS-CFX, Ind. Eng. Chem. Res. 48 (2009) 8159-8171.
[16] V. Matoušek, Concentration profiles and solids transport above stationary deposit in enclosed conduit, J. Hydraul. Eng.-ASCE 135 (2009) 1101-1106.
[17] J.M. Furlan, V. Mundla, J. Kadambi, N. Hoyt, R. Visintainer, G. Addie, Development of A-scan ultrasound technique for measuring local particle concentration in slurry flows, Powder Technol. 215-16 (2012) 174-184.
[18] J. Capecelatro, O. Desjardins, Eulerian-Lagrangian modeling of turbulent liquid-solid slurries in horizontal pipes, Int. J. Multiphas. Flow 55 (2013) 64-79.
[19] M.C. Roco, C.A. Shook, Critical deposit velocity in slurry flow, AlChE J. 31 (1985) 1401-1404.
[20] D.R. Kaushal, Y. Tomita, Prediction of concentration distribution in pipeline flow of highly concentrated slurry, Particul. Sci. Technol. 31 (2013) 28-34.
[21] D.R. Kaushal, Y. Tomita, An improved method for predicting pressure drop along slurry pipeline, Particul. Sci. Technol. 20 (2002) 305-324.

[22] D.R. Kaushal, K. Sato, T. Toyota, K. Funatsu, Y. Tomita, Effect of particle size distribution on pressure drop and concentration profile in pipeline flow of highly concentrated slurry, Int. J. Multiphas. Flow 31 (2005) 809-823.
[23] D.R. Kaushal, Y. Tomita, Solids concentration profiles and pressure drop in pipeline flow of multisized particulate slurries, Int. J. Multiphas. Flow 28 (2002) 1697-1717.
[24] P.D. Thorne, D.M. Hanes, A review of acoustic measurement of small-scale sediment processes, Cont. Shelf Res. 22 (2002) 603-632.
[25] H.P. Rice, Transport and deposition behaviour of model slurries in closed pipe flow, Ph.D. thesis, University of Leeds, 2013.
[26] D. Hurther, P.D. Thorne, M. Bricault, U. Lemmin, J.-M. Barnoud, A multi-frequency Acoustic Concentration and Velocity Profiler (ACVP) for boundary layer measurements of fine-scale flow and sediment transport processes, Coast. Eng. 58 (2011) 594-605.
[27] A. Downing, P.D. Thorne, C.E. Vincent, Backscattering from a suspension in the near field of a piston transducer, J. Acoust. Soc. Am. 97 (1995) 1614-1620.
[28] M.A. Ainslie, J.G. McColm, A simplified formula for viscous and chemical absorption in sea water, J. Acoust. Soc. Am. 103 (1998) 1671-1672.
[29] P.D. Thorne, R. Meral, Formulations for the scattering properties of suspended sandy sediments for use in the application of acoustics to sediment transport processes, Cont. Shelf Res. 28 (2008) 309-317.
[30] P.D. Thorne, D. Hurther, B.D. Moate, Acoustic inversions for measuring boundary layer suspended sediment processes, J. Acoust. Soc. Am. 130 (2011) 1188-1200.